THE ASTRONOMICAL JOURNAL VOLUME 111, NUMBER 6 JUNE 1996

HUBBLE SPACE TELESCOPE WFPC2 IMAGING OF M16: PHOTOEVAPORATION AND EMERGING YOUNG STELLAR OBJECTS[1]

J. JEFF HESTER,[2] PAUL A. SCOWEN,[2] RAVI SANKRIT,[2] TOD R. LAUER,[3,4] EDWARD A. AJHAR,[3,4] WILLIAM A. BAUM,[5] ARTHUR CODE,[6] DOUGLAS G. CURRIE,[7] G. EDWARD DANIELSON,[8] SHAWN P. EWALD,[8] SANDRA M. FABER,[9] CARL J. GRILLMAIR,[9] EDWARD J. GROTH,[10] JON A. HOLTZMAN,[11] DEIDRE A. HUNTER,[12] JEROME KRISTIAN,13 ROBERT M. LIGHT,[14] C. ROGER LYNDS,[3,4] DAVID G. MONET,[15] EARL J. O'NEIL, JR.,[3,4] EDWARD J. SHAYA,[7] KENNETH P. SEIDELMANN,[16] AND JAMES A. WESTPHAL[8]

Received 1995 September 21; revised 1996 February 20

ABSTRACT

We present *Hubble Space Telescope* WFPC2 images of elephant trunks in the H II region M16. There are three principle results of this study. First, the morphology and stratified ionization structure of the interface between the dense molecular material and the interior of the H II region is well understood in terms of photoionization of a photoevaporative flow. Photoionization models of an empirical density profile capture the essential features of the observations, including the extremely localized region of [S II] emission at the interface and the observed offset between emission peaks in lower and higher ionization lines. The details of this structure are found to be a sensitive function both of the density profile of the interface and of the shape of the ionizing continuum. Interpretation of the interaction of the photoevaporative flow with gas in the interior of the nebula supports the view that much of the emission from H II regions may arise in such flows. Photoionization of photoevaporative flows may provide a useful paradigm for interpreting a wide range of observations of H II regions. Second, we report the discovery of a population of small cometary globules that are being uncovered as the main bodies of the elephant trunks are dispersed. Several lines of evidence connect these globules to ongoing star formation, including the association of a number of globules with stellar objects seen in IR images of M16 or in the continuum *HST* images themselves. We refer to these structures as evaporating gaseous globules, or "EGGs." These appear to be the same type of object as the nebular condensations seen previously in M42. The primary difference between the two cases is that in M16 we are seeing the objects from the side, while in M42 the objects are seen more nearly face-on against the backdrop of the ionized face of the molecular cloud. We find that the "evaporating globule" interpretation naturally accounts for the properties of objects in both nebulae, while avoiding serious difficulties with the competing "evaporating disk" model previously applied to the objects in M42. More generally, we find that disk-like structures are relatively rare in either nebula. Third, the data indicate that photoevaporation may have uncovered many EGGs while the stellar objects in them were still accreting mass, thereby freezing the mass distribution of the protostars at an early stage in their evolution. We conclude that the masses of stars in the cluster environment in M16 are generally determined not by the onset of stellar winds, as in more isolated regions of star formation, but rather by disruption of the star forming environment by the nearby O stars.

---

[1]Based on observations with the NASA/ESA *Hubble Space Telescope,* obtained at the Space Telescope Science Institute, which is operated by AURA Inc., under NASA contract 5-26555.

[2]Department of Physics and Astronomy, Arizona State University, Tempe, Arizona 85287.
[3]Kitt Peak National Observatory, National Optical Astronomy Observatories[10], Box 26732, Tucson, Arizona 85726.
[4]Operated by the Association of Universities for Research in Astronomy, Inc. under cooperative agreement with the National Science Foundation.
[5]Department of Astronomy, FM-20, University of Washington, Seattle, Washington 98195.
[6]Washburn Obs., Dept. of Astronomy, 475 N. Charter St., Madison, Wisconsin 53706.
[7]Department of Physics and Astronomy, University of Maryland, College Park, Maryland 20742.
[8]Division of Geological and Planetary Sciences, California Institute of Technology, 170-25, Pasadena, California 91125.
[9]UCO/Lick Observatory, Board of Studies in Astronomy and Astrophysics, University of California, Santa Cruz, California 95064.
[10]Department of Physics, Princeton University, Princeton, New Jersey 08544.
[11]Department of Astronomy, New Mexico State University, Las Cruces, New Mexico 88003.
[12]Lowell Observatory, 1400 W. Mars Hill Road, Flagstaff, Arizona 86001.
[13]The Observatories, Carnegie Institution of Washington, 813 Santa Barbara St., Pasadena, California 91101-1292.
[14]IPAC, Caltech, 100-22, Pasadena, California 91125.
[15]US Naval Observatory, P.O. Box 1149, Flagstaff, Arizona 86002-1149.
[16]US Naval Observatory, 3450 Massachusetts Ave., NW, Washington DC.

 0004-6256/96/111(6)/2349/12/$6.00

1. INTRODUCTION

The first *Hubble Space Telescope* images of an H II region—M42 (Hester *et al.* 1991a)—showed the interface between the H II region and the molecular cloud to be remarkably thin; a significant fraction of the emission from low ionization lines originates from within a few hundred AU of the H II region/molecular cloud interface. The images also clearly showed the stratification of the ionization structure of the gas near the interface. This stratified structure was further discussed by Hester (1991), who interpreted it in terms of photoionization of the photoevaporative flow away from the interface.

Photoevaporation of molecular material by ultraviolet radiation from massive stars is an old problem, dating back to the seminal work by Oort & Spitzer (1955) and further developed by Kahn (1969), Sandford *et al.* (1982), and others. More recently photoevaporation of clouds has been studied by Bertoldi (1989) and Bertoldi & McKee (1990), who were interested in H II region evolution as well as radiatively driven implosion as a mechanism of induced star formation. Photoevaporation might be an especially important process in the context of blister models of H II regions. It has been clear for some time that H II regions seen in visible light are generally blister-like structures which have broken out of the molecular clouds which gave birth to the exciting stars (e.g., Zuckerman 1973; Pankonin *et al.* 1979; Peimbert 1982; Baldwin *et al.* 1991; Rubin *et al.* 1991). Hester (1991) emphasized that the entire surface of the blister is a photoevaporative flow, and suggested that photoionized photoevaporative flows might account for much of the emission from H II regions. In this view a better understanding of photoevaporative flows might prove to be important in interpreting a wide range of observations of H II regions.

Unfortunately, M42 is not an ideal location for studying photoevaporative interfaces. The interface in M42 is seen mostly face-on, so the observer is generally looking *through* the structure rather than across it. Even interpretation of the Orion "bar" is complicated by projection effects. A much less ambiguous viewing geometry can be found in the H II region M16. M16 (NGC 6611, S49, or more popularly, the "Eagle Nebula") is part of a larger region of star formation, much of which is still embedded within the molecular cloud (e.g., Goudis 1976). M16 is best known for several prominent "elephant trunk" structures. These protrusions began as overdense regions in the molecular cloud, which evolved into the forms seen under the combined effects of photoevaporation and instabilities in the rocket-effect-driven flows that shape the evolving H II region (e.g., Giuliani 1979). In ground based images the heads of these structures appear as limb-brightened arcs, and are bright in emission from both low and high ionization species. The convex surfaces of the elephant trunks in M16 provide an ideal viewing geometry in which the H II region/molecular cloud interface is seen in tangency against a relatively smooth background, allowing for a minimum of confusion due to background and projection effects. This more favorable geometry allows a clear look at the cross section of the flow away from the interface—the same sort of flow that should be present everywhere along the photoionized face of the molecular cloud.

In addition, M16 is a region of active star formation, and contains many young low and intermediate mass pre-main-sequence stars (Hillenbrand *et al.* 1993). The elephant trunk structures in M16 are the result of the interaction of massive stars with their environment, but in turn are themselves sites of star formation. By studying the structure of the interface between the elephant trunks and H II region we might hope to better understand the effect of massive stars on their environment, and in particular the effect that they have on continuing star formation.

In this paper we present new *Hubble Space Telescope* Wide Field and Planetary Camera 2 (WFPC2) observations of the photoevaporative interface along the surfaces of the elephant trunks in M16. In Sec. 2 we present the observations. The photoevaporative interface is discussed in Sec. 3. We report the discovery of a population of small cometary globules, a number of which are known to be associated with young stellar objects (YSOs). These evaporating gaseous globules, or EGGs, are discussed in Sec. 4. The effect of photoevaporation on star formation in M16 is discussed in Sec. 5. A brief summary and a few concluding remarks are given in Sec. 6.

2. OBSERVATIONS AND RESULTS

2.1 Observations

Figure 1 (Plate 133) shows an Hα image of M16 taken with the Wide Field PFUEI on the Palomar 1.5 m telescope (Hester *et al.* 1991b). M16 is famous for the large elephant trunk features seen protruding into the interior of the nebula. The small box shows the region of the nebula which was imaged using the *Hubble Space Telescope* Wide Field and Planetary Camera 2. The WFPC2 has been described by Trauger *et al.* (1994). The WFPC2 has four independent CCD cameras that image adjacent fields of view. Each of these cameras records its image onto a Loral 800 × 800 CCD. Three of these cameras (the Wide Field Cameras) have an image scale of 0.″1 per pixel. The remaining camera (the Planetary Camera) has an image scale of 0.″046 per pixel.

Two exposures were obtained in each of four filters: F656N (Hα λ6563), F502N ([O III] λ5007), F673N ([S II] ($\lambda\lambda$ 6717,6731), and a largely line free continuum filter (F547M). The images were taken on 1 April, 1995. Integration times were 2 × 1100 seconds for Hα, [S II], and [O III], and 2 × 140 seconds for F547M. The images were reduced using standard procedures as described in Holtzman *et al.* (1994). The two exposures in each filter were combined using an algorithm that rejects cosmic rays by comparing the difference between the two exposures with the computed noise. Mosaics of the combined images were constructed by resampling the data onto a common grid using the astrometric solution given by Holtzman *et al.* (1994). Figures 2, 3,

and 4 (Plates 134, 135, and 136) show the Hα, [S II], and [O III] images, respectively. The displays employ a square root stretch, allowing both faint and brighter features to be seen in the same figure. Figure 5 shows a color composite of the images, with [S II] shown as red, Hα as green, and [O III] as blue.

2.2 Basic Geometry

The distance to M16 is approximately 2 kpc (Humphreys 1978; Hillenbrand *et al.* 1993). At this distance, $1'' = 3\times10^{16}$ cm, so one WFC pixel is 3×10^{15} cm on a side, while a PC pixel is 1.3×10^{15} cm (90 AU) on a side. The field of view of the WFPC2 covers the three most prominent elephant trunk features in nebula. Moving from northeast to southwest (left to right across the WFPC2 image), we refer to these structures as columns I, II, and III, respectively. The principle sources of ionizing radiation in M16 are the stars located 3.5 or about 6×10^{18} cm to the northwest of the heads of the elephant trunks. (The ionizing radiation is coming from "above" in the WFPC2 images shown in Figs. 2 through 4 and Fig. 5 (Plate 137).) The elephant trunk structures and the ionizing stars appear to fall close to the plane of the sky. Column I shows emission all along its front face, implying that it is being illuminated by the ionizing stars, and so is presumably somewhat behind the ionizing stars. Conversely, columns II and III are seen almost exclusively as extinction features against the nebular background. They are presumably illuminated on their far sides, and so are somewhat in front of the ionizing stars.

3. PHOTOEVAPORATION

3.1 The Photoevaporative Flow in M16

The WFPC2 images of M16 show clear morphological evidence of photoevaporation. The band of Hα and [O III] emission surrounding the upper portions of all three columns shows clear striations pointing normal to the interface, where photoevaporated material is streaming away from the molecular cloud into the interior of the H II region. The visual appearance is much like that of *Giotto* images of comet Halley, which showed similar striations pointing outward from locations from which volatile materials were being driven off of the nucleus of the comet. This structure can be seen in greater detail in Fig. 6 (Plate 138), which shows an enlargement of the Hα image of the head of column I.

The morphology of the emission has a number of implications about the properties of the flow. The fact that the striations in M16 point normally away from the interface indicates that the pressure gradient driving the flow remains normal to the interface, regardless of the angle of incidence of the ionizing radiation or orientation with respect to the rest of the H II region (cf. Dyson 1973). The implication is that energy deposition at the interface itself is more important in the dynamics of the flow than either energy deposition in the outer parts of the flow or interaction of the flow with material in the interior of the H II region; neither of these effects cause the flow lines in the photoevaporative flow to be diverted by much. This is consistent with earlier work on photoevaporation and the related "rocket effect" (e.g., Oort & Spitzer 1955; McKee *et al.* 1984). The extremely thin nature of the acceleration region can also be seen in Fig. 4 in Bertoldi (1989).

3.2 Ionization Structure of the Photoevaporative Flow

3.2.1 Observed structure

The differences among the images in the three emission lines is striking. The edges of the elephant trunks are seen in sharp relief in the [S II] image (Fig. 3); [S II] emission is strongly concentrated in an extremely sharp zone right at the edge of the dense molecular material. In contrast, [O III] emission forms more diffuse halos surrounding the elephant trunks (Fig. 4). The bright rim that dominates the [S II] image is all but missing in [O III]. Rather, in [O III] we see a sharp edge of extinction at the same location as the bright [S II] rim. Hα is intermediate between [S II] and [O III] (Fig. 2). The halo seen in [O III] is present in Hα as well. In addition to the halo, Hα also shows a bright rim at the interface as well, like that seen in [S II]. However, the Hα rim is neither as narrow nor as prominent as the [S II] rim, and the Hα peak is displaced somewhat away from the molecular cloud from the [S II] peak.

This stratified structure can also be seen in Fig. 7a, which shows profiles of the three lines along a cut taken through the evaporative flow normal to the tip of column II in the PC. Moving from the elephant trunk outward, the rise of the [S II] profile is unresolved at a FWHM resolution of $\sim$ 200 AU. It then falls exponentially with a $1/e$ scale height of $\sim1.9\times10^{16}$ cm. The Hα profile rises as rapidly as well, but peaks $\sim$ 100 AU outside of the [S II] peak, then falls with a scale height of about twice that of [S II]. The [O III] profile rises more slowly than the lower ionization lines, reaching a broader peak about 2×10^{16} cm outside of the [S II] peak, then slowly falls until it blends with the background a few $\times10^{17}$ cm from the surface of the cloud.

3.2.2 Photoionization models

The extremely thin low ionization zone, the density and pressure gradient implied by the steep Hα profile, and the ionization structure normal to the interface seen in M16 are all as expected from photoionization of a photoevaporative flow (cf. Fig. 7a with Fig. 4 from Hester 1991 and Fig. 6 from Bertoldi 1989). To investigate the structure of this interface we assumed that the density distribution of the flow away from the surface is proportional to the square root of the Hα surface brightness up to the ionization edge at the interface itself. This assumption overestimates the density and volume emissivity of regions further from the interface, where the line of sight through the emitting region is longer than the line of sight through the bright [S II] rim. However, this procedure should be acceptable in the region of particular interest very near the interface. A polynomial fit was used to extrapolate this density profile further into the cloud to allow calculation of the emission from the [S II] zone.

Using the stellar census of M16 from Hillenbrand *et al.* (1993), the conversion between mass and spectral type from Howarth & Prinja (1989), and total ionizing flux versus stellar type from Osterbrock (1989), we estimate that half of the

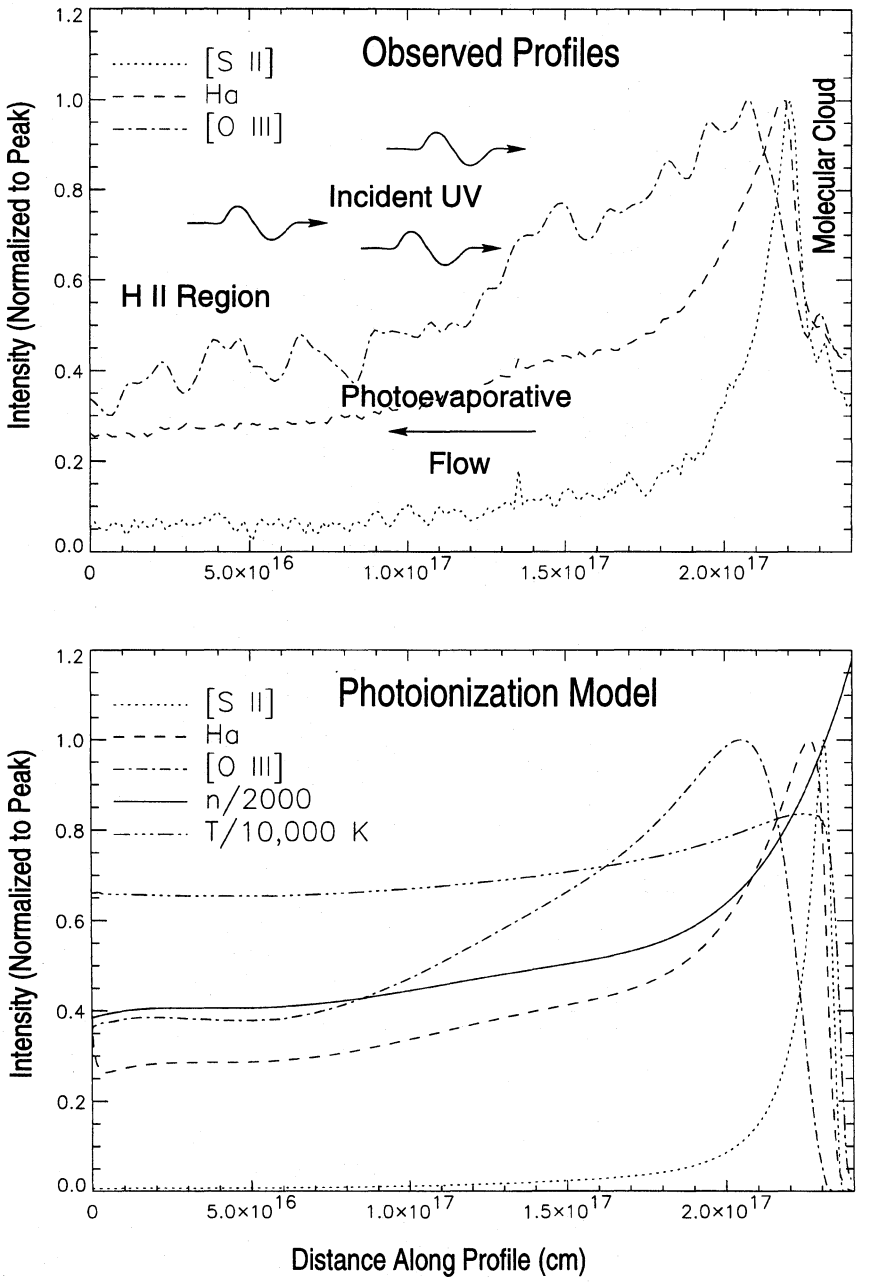

FIG. 7. (a) Observed profiles of the Hα, [S II], and [O III] emission along a cut taken normal to the photoevaporative interface at the tip of column II in M16. The profiles were extracted from the Planetary Camera image. The FWHM resolution of the [S II] and Hα profiles is $\sim 2.7\times10^{15}$ cm, or 180 AU. The [O III] profile was lightly filtered and smoothed to reduce noise. (b) Profile showing a model calculation of the ionization structure of the photoevaporative interface. The molecular cloud is to the right and ionizing radiation is incident from the left. The density profile was assumed to be proportional to the square root of the observed Hα brightness. While this assumption is probably valid near the sharp edge, it overestimates the density in the outer parts of the flow due to projection effects.

ionizing radiation in M16 comes from a single O3–4 star. The remaining ionizing radiation mostly comes from three stars with spectral type O5–6. We estimate that the total ionizing flux for the nebula is $\sim 2\times10^{50}$ photons per second, with the ionizing sources located a distance of 6×10^{18} cm from the elephant trunks. We approximated this spectrum using a Kurucz (1991) model with T=50,000 K. We then used CLOUDY84 (Ferland 1993) to compute the expected ionization structure of the interface, adjusting the normalization of the density profile until the position of the ionization edge matched the observations.

Figure 7b presents the result of this calculation. The agreement between observations and the model is remarkably good. In particular the sharpness of the [S II] zone and the offsets between the peaks of the [S II], Hα, and [O III] zones reproduce the observed profiles very well. As part of

the modeling we investigated the sensitivity of the profiles to variations in the model parameters. We found that the details of the ionization structure, and in particular the location of the peak of the [O III] zone, were extremely sensitive to the shape of the assumed ionizing spectrum. For a given profile, too hard an ionizing spectrum drove the [O III] zone too far into the dense portions of the flow, while too soft a spectrum gave [O III] emission only in the outermost parts of the evaporative halo.

The observed brightness of the photoevaporative flow is also quantitatively consistent with this model. The heads of the three main columns are roughly hemispherical, with the geometry of the head of column II being especially simple. Allowing for ~ 2 magnitudes of extinction (Chini & Krügel 1983), the Hα emission measure in the bright rim at the tip of column II has a characteristic value of around 3×10^5 cm^{-6} pc. We estimate from the observed geometry that the line of sight of through the bright rim is about 2″ or 0.02 pc, which gives a typical density of ~ 4000 cm^{-3} at the head of the column. This is in reasonable agreement with the density of ~ 2000 cm^{-3} at the peak of the Hα profile in the photoionization model.

The structure of the photoevaporative flow can also be compared directly with the calculations of Bertoldi (1989) and Bertoldi & McKee (1990). The radius of curvature at the head of column II is 0.04 pc, and the column is located at a distance of approximately 2 pc from the ionizing stars. Using these values in equation 3.23 from Bertoldi & McKee (1990), and dividing by 2 to account for the fact that ram pressure is included in that expression, gives a predicted thermal pressure at the tip of column II of $p/k=1.4\times10^8$ cm^{-3} K. This is only about a factor of 2 larger than the observed value of $p/k=6\times10^7$ cm^{-3} K. This should probably be considered good agreement given the uncertainties in the observational value and the fact that M16 is far more extreme a case than any considered by Bertoldi. Substituting the relevant parameters into the expression for the photoevaporation parameter (Bertoldi 1989) gives $\psi=10^4$, which is a factor of 30 more extreme than the cases considered in that work.

3.3 H II Regions as Photoevaporative Flows

3.3.1 Photoionized photoevaporative flows as well determined physical structures

The work presented here shows that the rapidly varying ionization structure at the interface between the interior of M16 and the dense elephant trunks can be quantitatively understood as the photoionization of a photoevaporative flow extending from the surface of the molecular cloud out to a distance of at least several $\times10^{17}$ cm from the interface. We stress that the density profile, the dynamical structure of the flow, and the ionization structure are determined by the *same* set of physical parameters. The implication is that the emission from photoevaporative flows might be modeled in a way that is analogous to the way in which radiative shocks are modeled (e.g., Cox 1972; Raymond 1979; Dopita 1977; Shull & McKee 1979). Whereas with shocks the relevant parameters include shock velocity, preshock density, magnetic field strength, and swept up column, in the case of photoevaporative flows the relevant parameters include the density of the molecular cloud, the ambient pressure of the medium into which the flow is moving, and the shape and strength of the radiation field. The fact that easily observed quantities such as the offset in the peaks of different ionization zones are seen here to be strongly dependent on these parameters suggests that this technique has very good potential for providing physical diagnostics of such interfaces.

3.3.2 Significance of emission from the photoevaporative flow

The above conclusion seems secure for photoevaporative flows, *per se*, but it is interesting to speculate further about the significance of such flows in determining the overall emission from H II regions. As noted, Hester *et al.* (1991a) found that the same sort of sharp, stratified structure seen in M16 is present along the face of the blister in M42. This supports the view that emission from near the wall of a blister H II region itself is best described as a photoionized photoevaporative flow. Hester *et al.* (1991b) see what appear at low resolution to be similar structures throughout ground based observations of 30 Galactic H II regions, suggesting that the phenomenon is fairly general.

Having argued that the edges of blister H II regions are photoionized photoevaporative flows, the next question is how much of the overall emission from an H II region comes from such flows. Hester (1991) argues that such flows may actually dominate the emission from blister H II regions. We will leave to later papers the task of developing a broader observational base of evidence supporting this interpretation. However, it is worth noting that in the context of blister H II region models the low filling factors of H II regions (e.g., Kennicutt 1984) require that emission be concentrated relatively near the boundary of the molecular cloud—in the zone that we suggest is best understood as a photoionized photoevaporative flow.

We can clarify this idea by considering a situation in which a photoevaporative flow comes off of the surface of a molecular cloud, and then undergoes a shock transition when the ρv^2 of the flow is balanced by the "ambient" pressure in the interior of the H II region. (In the absence of such a shock, the interior of the H II region is nothing more than the extension of the photoevaporative flow itself.) Stated simply, if most of the emission from the H II region arises between the photoevaporative interface and this shock, then our suggestion is correct. If, on the other hand, the majority of the emission from the H II region occurs beyond this shock, then our suggestion is not valid. The location of the shock then becomes the crucial question in assessing this idea.

3.3.3 The flow shock in M16 and the "ambient" density in the H II region

In the *HST* image of M16 the well-defined striations in the flow extend smoothly away from columns out to distances of at least 4×10^{17} cm from their surfaces, and we see no evidence of structure suggestive of a shock out to the edges of the field of view of the WFPC2. Looking at the ground based image in Fig. 1 the photoevaporative flow can be seen to extend further out still. The closest features that might be ascribed to a shock in the photoevaporative flow are a series of faint filaments, concave toward the elephant

trunks, located about 30″ to the northwest of the upper edge of the PC1 field of view. This observation can be used to place a limit on the density in the interior of the H II region.

Returning to the case of column II, outside of the acceleration zone the ram pressure should fall off approximately as $1/r^2$ because of the divergence of the flow. Since it is the pressure at the ionization front that drives the photoevaporative flow, conservation of momentum requires that $\rho v^2 \approx P_{if}(r_0/r)^2$, where r_0 is the radius of curvature of the tip of the column, r is the distance away from the center of curvature, P_{if} is the pressure at the ionization front, and ρv^2 is the ram pressure of the flow. The flow will shock when it diverges to the point that $\rho v^2 \approx P_{\rm H\,II}$, where $P_{\rm H\,II}$ is the ambient pressure in the H II region. Since T≈8000 K everywhere in the ionized gas, these equations simplify to state that the diverging flow will shock when $n_{\rm H\,II} \approx n_{if}(r_0/r)^2$.

If the feature seen in the ground-based image to the northwest of column II is taken to be the shock in the photoevaporative flow, then we have $r \approx 1.4\times10^{18}$ cm and $r_0 \approx 1.2\times10^{17}$ cm. Using $n_{if}=4000$ cm^{-3} then gives an estimate of $n_{\rm H\,II} \approx 29$ cm^{-3} for the "ambient" density in the interior of the H II region. Taking a line of sight distance of ~ 2 pc through the interior of the nebula, this implies that the emission measure from the "ambient" interior of the nebula (that is, the region which is not part of the photoevaporative flow) is only about 1700 cm^{-6} pc. This is certainly consistent with our suggestion that the "ambient interior" of the H II region makes little contribution to the observed emission from the nebula, which typically has an extinction corrected emission measure of well over 10^4 cm^{-6} pc.

We have used the properties of the photoevaporative flow away from the surface of the elephant trunks in M16 to argue that emission from the nebula as a whole is dominated by the photoionized photoevaporative flow from the wall of the blister. If after consideration of a broader base of evidence a general conclusion is reached that emission from H II regions is dominated by photoionized photoevaporative flows, this could provide a powerful and well defined physical paradigm for interpretation of observations of H II regions. Drawing again on the analogy with the application of shock models, H II region models based on photoionized photoevaporative flows might prove especially useful for interpretation of more distant H II regions where the stratification of the photoevaporative flow is unresolved, but where other observations constrain the parameters of photoevaporative models.

4. EVAPORATING GASEOUS GLOBULES

We might expect to see the small scale structure within the main elephant trunks to be revealed as the elephant trunks are eroded away by photoevaporation. Indeed, the *HST* images show numerous fascinating small-scale structures along the photoevaporative surfaces of the elephant trunks in M16. Figure 10 shows a number of these interesting features. By far the largest class of noteworthy objects are the many small cometary globules protruding from the surfaces of the three columns. There are several regions

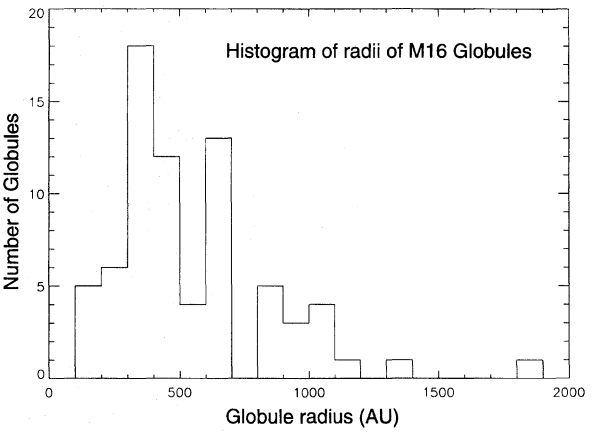

FIG. 9. A histogram of measured radii of the globules shown in Fig. 8.

where these globules are concentrated (i.e., where the photoevaporative surface of the elephant trunks are very irregular), indicating that the molecular cloud was very clumpy at these locations. Examples of such regions include the heads of columns I and II and the lower right part of column I. In many other locations the photoevaporative interface is very smooth. Figure 6 shows an enlargement of the head of column I in which numerous globules can be seen, including a number of small globules that are more difficult to pick out in the lower resolution reproductions. The morphologies of these globules range from "bumps" in the outline of columns, to elongated conical or drop-like structures protruding from the columns, to a few objects that are completely detached from the surface of the columns.

Identifying and measuring these globules is very subjective, especially near the resolution limit of the images. Given this subjectivity it seems most appropriate to consider the properties of all small bumps along the surfaces of the elephant trunks (as well as a few detached objects). Working by hand we identified 73 features, indicated in a high pass filtered Hα image in Fig. 8 (Plate 139), and measured their approximate sizes. The smallest of the features detected have radii of approximately 150 AU, which is set by the resolution of the images, and the largest are over 1000 AU in radius. A histogram of the distribution of the radii of these objects is presented in Fig. 9.

4.1 EGGs

The morphology of these objects and their distribution near the surface of the molecular cloud suggest that they are globules of dense gas that are being photoevaporated more slowly than their lower density surroundings, and so are left behind as the gas around them is driven off. In short, they are the result of substructure within the elephant trunks that is uncovered as the elephant trunks themselves are photoevaporated and/or pushed away by the photoevaporation-driven rocket effect.

Most of these globules are conical or have elongated necks that tie them back to the surfaces of the elephant trunks. These necks point directly away from the ionizing stars, indicating that they are probably columns of gas that

have not evaporated due to shadowing behind the dense clumps at their heads. The fact that few of these structures are totally detached from the interface and that none are seen further than about 10^{17} cm from the interface indicates that these are relatively short-lived structures. Assuming a propagation speed for the photoionization front of order 5 km s^{-1} (Bertoldi 1989), the distribution of these objects suggests that few survive longer than about 10^4 years after emerging from within the molecular cloud. This is comparable to photoevaporative time scales for small nebular globules calculated by various authors (e.g., Bertoldi & Jenkins 1992).

In the spirit of previous names for small condensations in nebulae, we will refer to these features as Evaporating Gaseous Globules, or EGGs. Following the suggestion of the referee, we will refer to these objects using the nomenclature "M16-E*n*," where *n* is the EGG number shown in Fig. 8. This nomenclature can be extended to similar objects in other nebulae in the obvious way.

4.2 Star Formation in EGGs

M16 is the site of very active recent and ongoing star formation. The stellar content of M16 has recently been studied in the visible and infrared by Hillenbrand *et al.* (1993). The age of the massive stellar population in M16 is $\sim 1-2\times 10^6$ years, and the most massive star in the cluster has a mass of ~ 80 $M_\odot$. The ages of pre-main-sequence stars in M16 range from about 2.5×10^5 years to 1×10^6 years. In particular, M16 is noteworthy because of the large number of intermediate mass pre-main-sequence stars (3–8 $M_\odot$) found to be present.

By comparing the WFPC2 images with the K-band image used by Hillenbrand *et al.* (1993) we found several cases of EGGs that appear to be associated with YSOs with masses greater than 3 or 4 $M_\odot$. [One of these is the isolated source M16-E1 located just off of the upper left surface of column I and shown in Fig. 10e. Also see the other examples in Fig. 10 (Plate 140).] There are several more ambiguous instances of such associations, as well as several regions (e.g., the top of column I) that are generally bright in K and also show concentrations of EGGs. We predict that a more complete census of YSOs in M16 (down to a fraction of a solar mass) would reveal additional examples of globules containing lower mass YSOs.

Visible stars can be seen to be associated with several EGGs directly from the WFPC2 images, sometimes appearing at or very near the tips of cometary structures, rather than embedded within the globules themselves. The best example of this is M16-E42, which can be seen in the lower right of the field shown in Fig. 10a. This is an elongated conical structure, 6×10^{16} cm long and about 200 AU in radius, with a bright star seen immediately at its tip. Another example of a cometary EGG with a star at its tip is M16-E31 (Fig. 10c). M16-E3 is a faint, detached globule containing a visible star. M16-E52 (Fig. 10d) is one of the few possibly disk-like structures seen, and has a faint continuum source at its center.

4.3 An Evolutionary Scenario for EGGs

As noted above, the observed properties of most EGGs leads to an obvious suggestion for how these structures evolve, which is similar to that considered by Bertoldi (1989). This scenario is depicted schematically in Fig. 11, where examples are presented of features in each phase of the evolution of an EGG. Most EGGs begin as dense condensations within the molecular cloud (Fig. 11a), many of which *may* have either contained YSOs already, or been well on their way toward forming them. These may be like the clumps required to explain observations of photodissociation regions (e.g., Tauber *et al.* 1994). When the photoevaporative front reaches a globule (Fig. 11b), the globule evaporates more slowly than its surroundings, and so begins to emerge as a bump on the side of the cloud. As the photoevaporation front continues to move through the larger cloud, this bump develops into an elongated structure, due to the shadowing effect of the globule and the evaporated material around it (Fig. 11c). Due to the presence of multiple ionizing sources and the diffuse radiation field within the nebula the tail of the structure is not completely shielded, and may eventually pinch off. (In M16 the ionizing sources are concentrated in one direction, and totally detached EGGs are relatively rare.) As the EGG has been evolving its cometary structure, however, the ionization front has been slowly working its way into the front face of the globule, and eventually any embedded star will be exposed at the tip of the EGG (Fig. 11d). Once the globule itself has been evaporated, the remaining tail should evaporate relatively quickly (not shown).

We emphasize that while we do not know what fraction of EGGs contain YSOs, we have unambiguous evidence that a few of them do. For those globules containing stellar objects, "EGG" is an especially apt term. These are EGGs in which embryonic stars formed and grew, and from which young stars are now emerging.

4.4 Comparison with Globules Seen in M42

In this section we consider the relationship between the M16 EGGs and other small nebular condensations such as those identified in radio continuum images of M42 (Churchwell *et al.* 1987), and later seen in *HST* images (Hester *et al.* 1991; O'Dell *et al.* 1993; O'Dell & Wen 1994). The objects in M42 have also been studied in the infrared (e.g., McCaughrean & Stauffer 1994), using adaptive optics (McCullough *et al.* 1995), and most recently at millimeter wavelengths (Mundy *et al.* 1995). These externally ionized cometary globules have been referred to using a number of terms, including "Partially Ionized Globules" or PIGs (Garay 1987), and "proplyds" (an acronym for "protoplanetary disks;" O'Dell *et al.* 1993), with each name implying something about the supposed structure of the objects. EGGs have a number of features in common with previously identified PIGs, proplyds, Bok globules, and other small nebular condensations. These objects are seen in similar environments, are externally ionized, and are sometimes associated with YSOs.

In particular, the M16 EGGs are very similar in appear-

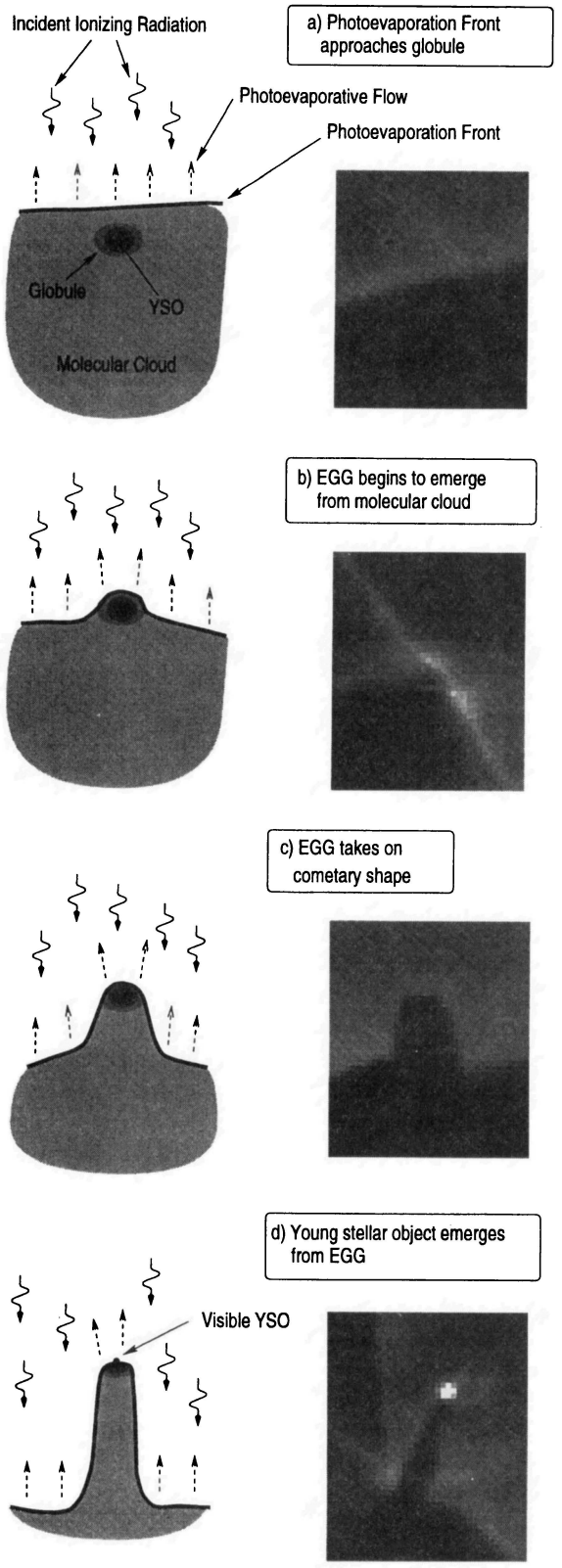

FIG. 11. An evolutionary scenario for the evaporating gaseous globules (EGGs) in M16. (a) A dense globule (which may contain a YSO) is embedded in a molecular cloud. (b) The globule survives against photoevaporation for longer than its surroundings. (c) This, combined with shadowing by the globule, leads to the formation of a cometary structure. (d) If a YSO is embedded in the globule it will first be seen at the head of the structure. The images show examples of objects found in the M16 sample.

ance to the limb brightened, cometary globules seen in *HST* images of M42 (O'Dell *et al.* 1993; O'Dell & Wen 1994). The M16 EGGs differ from the objects seen in M42 primarily in size. The M16 objects have a characteristic radius of 3–400 AU, as compared with a representative size of around 200 AU for the objects in M42. However, this difference may be superficial. While M16 is five times further away than M42, preventing us from clearly seeing objects corresponding to the smallest of the M42 condensations, the size range of the M16 objects overlaps with the objects in M42. Also, McCollough *et al.* (1995) found that the sizes of the globules in M42 are roughly proportional to $d^{2/3}$, where d is the distance from the ionizing sources. They suggest that this is reasonable if the radii of the globules are determined by the point at which recombinations approximately balance ionizations. (A similar process is probably at work in M16. What is now the surface of an EGG was probably previously a contour in a smooth density distribution inside the larger cloud.) The M16 objects, located at a distance of 2–3 pc from the ionizing sources (as opposed to distances typically less than 1 pc for the objects in M42) fit nicely into this trend. The similar morphologies of the objects and environments in which they are found suggest that they are similar in origin as well. While an exact comparison between the two nebulae is probably not appropriate owing to the difference in ionizing sources, the M16 EGGs seem to fit reasonably well into the same population of objects as the nebular condensations in M42.

4.4.1 Overcoming past objections to evaporating globules

Our interpretation of the M16 EGGs as evaporating globules, and our suggestion that they may be similar to the objects seen in M42, reopens a debate about the nature of small nebular condensations. Churchwell *et al.* (1987) considered an evaporating globule model such as ours for the objects in M42, but rejected it on the basis of two specific arguments: the lifetimes of the globules, and their association with visible YSOs. Instead, they suggested that the Orion PIGs are evaporating disks. This idea has been elaborated on by various authors, including O'Dell and collaborators (O'Dell *et al.* 1993; O'Dell & Wen 1994), and McCollough *et al.* (1995).

The same difference in perspective between M16 and M42 that gave us a more informative look at photoevaporation also shows us why neither of the traditional objections to an evaporating globule picture are valid. In a paper discussing the evaporation of objects near πSco, Bertoldi & Jenkins (1992) insightfully state, "Unless we happen to observe the remains of larger clouds just before they are completely destroyed, it is hard to reconcile this disparity in time scales [between evaporation times of a few $\times 10^4$ years and the few $\times 10^6$ year age of the cluster], thereby posing a strong argument against the cloud model." A disk is needed, this argument says, to enlarge the reservoir of gas to be photoevaporated. But in M16, where we view these globules from the side and can see their relationship to the molecular cloud, we find that the "unless" in Bertoldi and Jenkins' statement is exactly what we *are* seeing. EGGs *do* only live for a few times 10^4 years, in agreement with evaporative

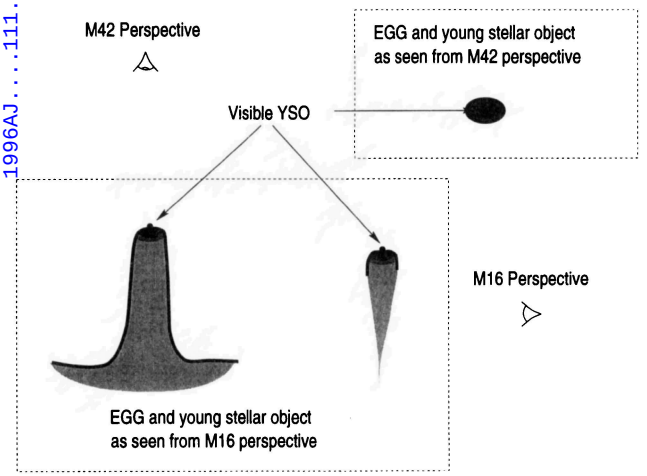

FIG. 12. A sketch showing how M16 EGGs and similar features seen in M42 differ principally in the direction from which they are observed.

Bertoldi and Jenkins go on to say, "A further argument against [the globule model] arises from the optical identification of several of the Orion PIGs with stellar-like objects." The argument is that stars would not be visible if they were embedded inside of globules, and therefore the material around them must actually be a disk. This objection is also answered by the edge-on perspective that we have on the globules in M16. The M16 data show that a star buried inside a globule is uncovered *from one side* long before the globule itself or its shadow tail are totally destroyed. Once a star is uncovered we view it *not* through the dense core of the EGG itself, but rather we see it through the evaporative flow surrounding the EGG. When viewed from a more face-on perspective, as is the case with the H II region/molecular cloud interface near the Trapezium in M42 (Fig. 12), we would see the stars *in projection* against the remains of the globule.

In this section we have shown that the historically cited reasons for favoring an evaporating disk model over an evaporating globule model are not valid, at least for M16 and M42. If viewed from more face-on, the evaporating globules in M16 would have just the properties that have lead previous authors to reject the evaporating globule picture in M42. If the evaporating disk model for these cometary globules is to be revived the burden of proof now lies with its proponents to present arguments that rely neither on time scales, nor on the morphology of the objects, nor on their association with visible stars.

4.4.2 Further difficulties with the evaporating disk model

There are additional difficulties that must be addressed by proponents of the evaporating disk model. The distribution of aspect ratios of the features seen in the *HST* images of M42 seems inconsistent with a random distribution of disk orientations. This is an argument against a picture in which PIGs are simply the ionized surfaces of disks. Rather, proponents of the evaporating disk picture propose that these objects are halos of material that have been evaporated from a embedded disks.

The most serious difficulty with the evaporating disk model arises from consideration of how disk evaporation is supposed to be driven. The evaporating disk model was originally suggested by Churchwell *et al.* (1987), who anticipated that PIGs would be ionized throughout their volume. In such a model, UV from the ionizing source would be able to penetrate the evaporated envelope and drive the disk evaporation. However, this model was shown to be incorrect by *HST* observations showing that the M42 PIGs are the externally ionized surfaces of *neutral* globules of gas. In response to these observations the evaporating disk model was modified (O'Dell *et al.* 1993; McCollough *et al.* 1995) by suggesting that the observed neutral material has been evaporated from an embedded disk by non-ionizing UV capable of penetrating the neutral envelope (see Fig. 6 in McCullough *et al.* 1995).

Consideration of the question of radiative transport shows that this variant of the evaporating disk model is not physically plausible. Using the same parameters for the globules used by McCullough *et al.* we find that any radiation reaching the disk from the outside must first propagate through a column of order 10^{22} cm^{-2} of neutral material. Assuming typical dust properties (e.g., Bohlin *et al.* 1978) and a standard extinction curve (Seaton 1979), this column implies that 2000 Å radiation will be attenuated by a factor of order 10^3 before reaching an embedded disk. The evaporating disk model is a steady state model in which the evaporative mass loss from the surface of the neutral envelope is balanced by the mass loss from the surface of the embedded disk. The question we raise is how can a small disk, buried behind several magnitudes of visible extinction, be evaporated rapidly enough to balance the mass loss from the larger surface of an envelope which is subjected to the full force of the radiation from the ionizing stars? The obvious answer is that it cannot.

This argument does *not* imply that there can be no disks embedded within the M16 EGGs or the Orion PIGs. Rather, it shows that external photoevaporation of embedded disks cannot be the source of the observed neutral globules. In the next section we consider the question of the widespread existence of disks more generally.

4.4.3 Disks are rare

While disks around stars in cluster environments are expected on theoretical grounds, observational evidence for them is scarce. Hillenbrand *et al.* (1993) noted that it is fairly rare to find infrared signatures of massive disks around intermediate and high mass stars in M16. Similarly, statistical limits of <0.03 $M_\odot$ for hypothetical disks in M42 (Mundy *et al.* 1995) are also close to being inconsistent with estimates of disk masses if disks are invoked to account for other observations (e.g., Stauffer *et al.* 1994). In the McCullough *et al.* (1995) version of the evaporating disk picture a significant fraction of stars in Orion should be seen in absorption *through* the disks—a result that may be inconsistent with the upper limit on absorbing columns inferred for the objects in M42 that they studied.

The globules in M42 have been cited as evidence for the formation of planetary systems (as the name "protoplanetary disk" implies), but reinterpretation of these features in light

of the M16 data suggests that the opposite may be the case. Perhaps the most compelling evidence *against* the widespread existence of massive disks inside of EGG-like objects are the *HST* images of M42 and M16. The best cases for disks in M42 are objects seen in absorption. In additional to a handful of isolated objects, a few Orion PIGs show what appear to be disk-like objects within them. This implies that if large disks are present, they can be seen. The fact that the majority of Orion PIGs do *not* show disk-like structures embedded within them might be taken as evidence that such structures are not present.

We can similarly address the question of disks in M16. If there are disks embedded within many of the EGGs, then when an EGG evaporates a disk should be left behind, and we should see these disks either in emission or as dark features against the background emission. There are three plausibly disk-like structures seen in the *HST* images of M16. Working in a high pass filtered version of the Hα images we found a small dark feature located near the top of the field of view, well above the head of column I. This object is 700 AU $\times$ <150 AU, and is about 80% as bright as the surrounding emission. (The fact that we do see such a relatively small, insubstantial object demonstrates that we are able to detect disks.) The second object is M16-E52, which is located along the left-hand edge of column II and is shown in Fig. 10d. This object is 1100 AU long $\times$ 500 AU wide, and has a faint extended continuum source at its center that is probably reflection nebulosity due to an embedded source. It is a very good candidate for a circumstellar disk surrounding a YSO. A third disk candidate is the small conical reflection nebula near the head of column II (see Fig. 10b). (This object was not given an EGG number, because it is purely a reflection nebulosity.) This object looks a great deal like objects such as HL Tau (Stapelfeldt *et al.* 1995), and might be understood as a disk and outflow cavity that are being uncovered as the surrounding material is photoevaporated. As this object is further uncovered it might go on to become an isolated disk-like structure such as M16-E52.

We conclude that we *can* see circumstellar disks that are left behind by photoevaporation in either nebula, but find that such objects are rare. We also find that YSOs can be associated with disks (e.g., M16-E52 and the object in Fig. 10b), but can also be associated with objects which do not obviously contain massive disks (e.g., M16-E1, M16-E32, and M16-E42). Hillenbrand *et al.* (1992) suggested that the scarcity of disks around massive stars might be because these disks are intrinsically short lived. Another possibility is that the early disruption of accretion in environments such as that studied in M16 might also influence disk evolution. Evidence that accretion onto YSOs is prematurely terminated in M16 will be discussed below in Sec. *5.2*.

4.4.4 Summarizing the M16/M42 comparison

We wish to be very explicit about the comparison we are making between M16 and M42. Most of the M16 EGGs appear to be the same sort of object as the luminous, limb brightened, often cometary globules originally labeled "proplyds" by O'Dell and coworkers. In contrast to the difficulties of the evaporating disk picture, our edge-on view of the globules in M16 leads to a description of these objects as evaporating globules, some of which surround YSOs. This picture naturally accounts for the observed properties of the objects seen in both nebulae.

In contrast, the single dark oval reported by O'Dell & Wen (1994), the dark ovals embedded within a few M42 PIGs, and a few other objects found in subsequent *HST* observations of M42 may be circumstellar disks. Two such objects are also seen in M16, one of which contains a star. However, these objects are relatively rare. While isolated disks may be the endpoint of the evolution of those EGGs which contain disks, the fact that we see relatively few such objects argues against the interpretation that EGGs generally evolve into bare, massive disks.

5. THE EFFECT OF O STARS ON STAR FORMATION

5.1 Triggered Star Formation versus Disruption of Star-Forming Clouds

The competing ideas of triggered star formation and star formation as a self-limiting process have been around for a long time. A good review of some of these ideas can be found in Elmegreen (1992). In particular, studies of bright-rimmed clouds containing infrared sources have been taken as evidence of star formation induced by radiatively driven implosion (e.g., Sugitani & Ogura 1994, and references therein). Recent work on the basic physics of photoevaporation and radiative implosion of clouds includes that of Bertoldi (1989) and Bertoldi & McKee (1990). Radiatively driven implosion may be important beyond the boundaries of bright H II regions, and may play a significant role in self-propagating star formation in galaxies (e.g., Cammerer & Shchekinov 1994).

The *HST* observations of M16 are of considerable interest because they may be offering us a close view of both the triggering and self-limiting aspects of this process. The elephant trunk structures in M16 are prominent members of the class of objects to which radiatively driven implosion models are applied. However, radiatively driven implosion did not lead to the formation of a single star as generally supposed. Rather, if this process played a role in triggering star formation in the M16 elephant trunks it was to hasten fragmentation and/or the collapse of existing clumps within the cloud, leading to the formation of the dense star-forming globules seen here as EGGs. On the other hand, the *HST* images offer direct evidence of the role of ionizing radiation in *limiting* the masses of stars currently forming in M16.

5.2 Limiting the Masses of Protostars

Shu and coworkers (e.g., Shu *et al.* 1987) make a compelling case that in regions of more isolated star formation such as the Taurus molecular cloud, the masses of stars are determined by the stars themselves. When a star reaches the point that it begins to produce a strong wind—an event that may be associated with the fact that the star is approaching the point of being able to support thermonuclear fusion in its core—that wind eventually stops further infall and dissipates the remainder of the cloud core from which the star formed. This is a very appealing picture, because it says that stars are

how big they need to be in order to be stars. An obvious question is whether this same basic picture also applies in cluster environments such as M16.

It is apparent that the stars forming within the M16 EGGs have accreted all of the material that they are going to. Photoevaporation of the cloud within which they were embedded has removed them from any reservoir of gas from which they could continue to draw. The question then is whether the YSOs within the EGGs had finished accreting mass before they were uncovered, or whether photoevaporation terminated accretion prematurely, and in so doing was responsible for determining the masses of these stars.

The Shu *et al.* picture of isolated star formation in which stellar winds terminate infall provides a way of addressing this question. As expected, YSOs forming in isolation often show ample evidence of environments that have been disrupted by outflows (e.g., numerous reviews including that of Reipurth 1991). In contrast, the EGGs in M16 are generally very smooth objects; in the locations where they are just emerging, they appear to join seamlessly with the larger molecular cloud of which they were a part. There is no observational reason to suggest that prior to being uncovered the M16 EGGs were anything other than smooth, spheroidal condensations embedded within the molecular cloud. Most of the objects in M16 show none of the sorts of structure typical of the disturbed environments surrounding stars forming in greater isolation.

There are a couple of exceptions to this statement. One is the small conical reflection nebula near the head of column II (Fig. 10b). Another is the left hand star in Fig. 10a, which could be interpreted as a YSO sitting in the midst of a small cavity. These objects may be the exceptions that prove the rule. If a YSO has disturbed its environment in the "usual" way then it leaves a signature that can be seen in the WFPC2 images of M16. The fact that most of the EGGs in M16 do *not* show such a disturbed structure is evidence that the stars they contain have yet to reach the point where they have strong winds. If Shu's ideas about the role of winds in determining the final masses of stars are correct, this means that the YSOs associated with the EGGs were still accreting mass when they were uncovered. In this view, photoevaporation is directly responsible for determining the masses of these stars. Further, the fact that there are over 70 EGGs but only two stars with evidence for outflow cavities would seem to indicate that external disruption of the star forming environment is the dominant process for determining stellar masses in M16.

It is possible in M16 that radiatively driven implosion and photoevaporation are responsible both for stimulating the formation of the new stars that we see, and in limiting the final masses that those *same* stars reach. It could be interesting to consider models of star formation that begin with radiatively driven implosion and subsequent fragmentation and collapse, then freeze the mass distribution of forming protostars with photoevaporation some characteristic time later.

Regardless of whether Shu's ideas are correct for stars in more isolated environments or whether we are correct in arguing that the stars in the EGGs have yet to blow strong winds, it is clear that photoevaporation of the molecular cloud is dispersing material that otherwise may have found its way onto protostars. While still in the molecular cloud, the cloud cores seen here as EGGs might have continued to grow. Once an EGG is uncovered, however, the mass of the protostar forming within it is set. Even if it turns out that many of the EGGs do *not* contain YSOs, this will remain a significant result. Such objects would be stars that "might have been," were it not for "premature" photoevaporation of the cloud from which there were forming. As noted by Hillenbrand *et al.* (1993), many of the YSOs in M16 "have still to accrete their full complement of natal material." Some of them never will.

6. SUMMARY AND CONCLUDING REMARKS

There are three main results of this work. First, we present observations of the morphology and the stratified ionization structure of the H II region/molecular cloud interface along the elephant trunk structures in M16. The observations are quantitatively understood as photoionization of a photoevaporative flow. This description may generalize to provide a physical paradigm which directly couples the physical, dynamical, and ionization properties of H II regions (Hester 1991). For example, Scowen *et al.* (1996), apply this same basic interpretation to the ionization structure seen in WFPC2 observations of 30 Doradus. Such a paradigm may remove much of the ambiguity normally present in H II region modeling, and suggests a way of calculating the observed structural and emission line properties of H II regions in terms of physical quantities such as the stellar content, the overall geometry of the region, the density of the molecular cloud, and the pressure of the medium surrounding the H II region. In future work we will investigate the larger implications of this paradigm.

Second, we report the discovery of a population of small cometary globules seen to be emerging from the photoevaporative interface itself. A number of these are known to contain YSOs. These objects, which can best be understood as evaporating gaseous globules or "EGGs," probably differ from similar limb-brightened cometary globules seen in M42 principally in the angle from which they are viewed. Unlike a number of recent papers, we find no need to invoke disks to explain observations of either population of objects. None of the traditional arguments used to motivate an evaporating disk model for these objects remain valid once the three dimension structure of the globules and their relationship with the molecular cloud are understood. Further, the evaporating disk model which is commonly applied to these objects is shown to be physically implausible. While a few disk-like structures *are* seen, these are rare.

Finally, M16 provides us with a look at the effect that massive stars can have on star formation in surrounding regions. We see little evidence for winds, jets, or other phenomena associated with outflows from YSO's. If such outflows are responsible for terminating infall in objects forming in isolation, the implication is that the masses of YSOs in M16 are often determined by a different process than stars in regions of isolated star formation. When an EGG is exposed by photoevaporation of its surroundings,

any YSO in its interior is removed from the reservoir of mass from which it was accreting material. This process can freeze the masses of protostars at an arbitrary time in their evolution.

In conclusion, the WFPC2 images of M16 are visually striking, and noteworthy from that perspective alone. They also provide a fascinating and enlightening glimpse of the physical processes at work in the interplay of massive stars and their surroundings.

It is a pleasure to thank and acknowledge C. F. McKee for a number of interesting comments and suggestions, and in particular for encouraging us to develop here several ideas originally left for subsequent papers. The authors would also like to thank L. Hillenbrand for making a representation of her IR images available for comparison with the WFPC2 data. Data reductions and analysis were carried out using software running within the IDL environment. This work has made use of the SIMBAD database, operated at CDS, Strasbourg, France. This work was supported by NASA Grant No. NAS-5-1661 to the WF/PC IDT and NASA Contract No. NAS-7-1260 to the WFPC2 IDT. This work was supported at ASU by NASA/JPL contracts 959289 and 959329 and Caltech contract PC 064528.

REFERENCES

Baldwin, J. A., Ferland, G. J., Martin, P. G., Corbin, M. R., & Cota, S. A. 1991, ApJ, 374, 580
Bertoldi, F. 1989, ApJ, 346, 735
Bertoldi, F., & Jenkins, E. B. 1992, ApJ, 388, 495
Bertoldi, F., & McKee, C. F. 1990, ApJ, 354, 529
Bohlin, R. C., Savage, B. D., & Drake, J. F. 1978, ApJ, 224, 132
Cammerer M. & Shchekinov, Y. 1994, A&A, 283, 845
Chini, R., & Krügel, E. 1983, A&A, 117, 289
Churchwell, E., Felli, M., Wood, D. O. S., & Massi, M. 1987, ApJ, 321, 516
Cox, D. P. 1972, ApJ, 178, 143
Dopita, M. A. 1977, ApJS, 33, 437
Dyson, F. 1973, A&A, 27, 459
Elmegreen, B. G. 1992 in Proceeding III Canary Island Winter School of Astrophysics, Star Formation in Stellar Systems, edited by G. Tenorio-Tagle, M. Prieto, and F. Sanchez (Cambridge University Press, Cambridge), p. 381
Ferland, G. J. 1993, University of Kentucky, Dept. of Physics & Astronomy Internal Report
Garay, G. 1987, RMxA&A 14, 489
Giuliani, J. L. 1979, ApJ, 233, 280
Goudis, C. 1976, Ap&SS, 41, 105
Hester, J. J. 1991, PASP, 103, 853
Hester, J. J., *et al.* 1991a, ApJ, 369, L75
Hester, J. J., Dufour, R. J., Parker, R. A. R., & Scowen, P. A. 1991b, BAAS, 23, 1364
Hillenbrand, L. A., Massey, P., Strom, S. E., & Merrill, K. M. 1993, AJ, 106, 1906
Hillenbrand, L. A., Strom, S. E., Vrba, F. J., & Keene, J. 1992, ApJ, 397, 613
Holtzman, J. A., *et al.* 1994, PASP, 107, 156
Howarth, I. D., & Prinja, R. K. 1989, ApJS, 69, 527
Humphreys, R. M. 1978, ApJS, 38, 309
Kahn, F. D. 1969, Physica, 41, 172
Kennicutt, R. 1984, ApJ, 287, 116
Kurucz, R. L. 1991, in Proceedings of the Workshop on Precision Photometry: Astrophysics of the Galaxy, edited by A. C. Davis Philip, A. R. Upgren, and K. A. James (Davis, Schenectady), p 27
McCaughrean, M. J., & Stauffer, J. R. 1994, AJ, 108, 1382
McCullough, P. R., Fugate, R. Q., Christou, J. C., Ellerbroek, B. L., Higgins, C. H., Spinhirne, J. M., Cleis, R. A., & Moroney, J. F. 1995, ApJ, 438, 403
McKee, C. F., Van Buren, D., & Lazareff 1984, ApJ, 278, L115
Mundy, L. G., Looney, L. W., & Lada, E. A. 1995, ApJ (submitted)
O'Dell, C. R., & Wen, Z. 1994, ApJ, 436, 194
O'Dell, C. R., Wen, Z., & Hu, X. 1993, ApJ, 410, 696
Oort, J. H., & Spitzer, L. 1955, ApJ, 121, 6
Osterbrock, D. E. 1989, The Astrophysics of Gaseous Nebulae and Active Galactic Nuclei (University Science Books, Mill Valley, California)
Pankonin, V., Walmsley, C. M., & Harwit, M. 1979, A&A, 75, 34
Peimbert, M. 1982, Ann. NY Acad. Sci., 395, 24
Raymond, J. C. 1979, ApJS, 39, 1
Reipurth, B. 1991, in The Physics of Star Formation and Early Stellar Evolution, edited by C. J. Lada and N. D. Kylafis (Kluwer, London), p. 497
Rubin, R. H., Simpson, J. P., Haas, M. R., & Erickson, E. F. 1991, ApJ, 374, 564
Sandford, M. T., Whitaker, R. W., & Klein, R. I. 1982, ApJ, 260, 183
Scowen, P. A., Hester, J. J., & Sankrit, R. 1996, in preparation
Seaton, M. J. 1979, MNRAS, 187, 73
Shu, F. H., Adams, F. C., & Lizano, S. 1987, ARA&A, 25, 23
Shull, J. M., & McKee, C. F. 1979, ApJ, 227, 131
Stapelfeldt, K. R., *et al.* 1995, ApJ (in press)
Stauffer, J. R., Prosser, C. F., Hartmann, L., & McCaughrean, M. J. 1994, AJ, 108, 1375
Sugitani, K., & Ogura, K. 1994, ApJS, 92, 163
Tauber, J. A., Tielens, A. G. G. M., Meixner, M., & Goldsmith, P. F. 1994, ApJ, 422, 136
Trauger, J. T., *et al.* 1994, ApJ, 435, L3
Zuckerman, B. 1973, ApJ, 183, 863

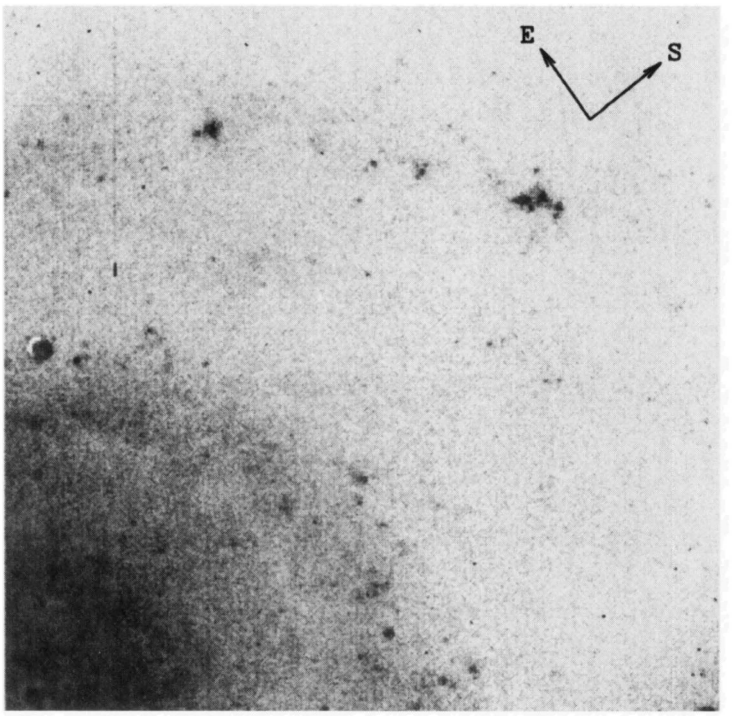

FIG. 1. The final *I* CCD frame of NGC 628.

Y. J. Sohn and T. J. Davidge (see page 2281)

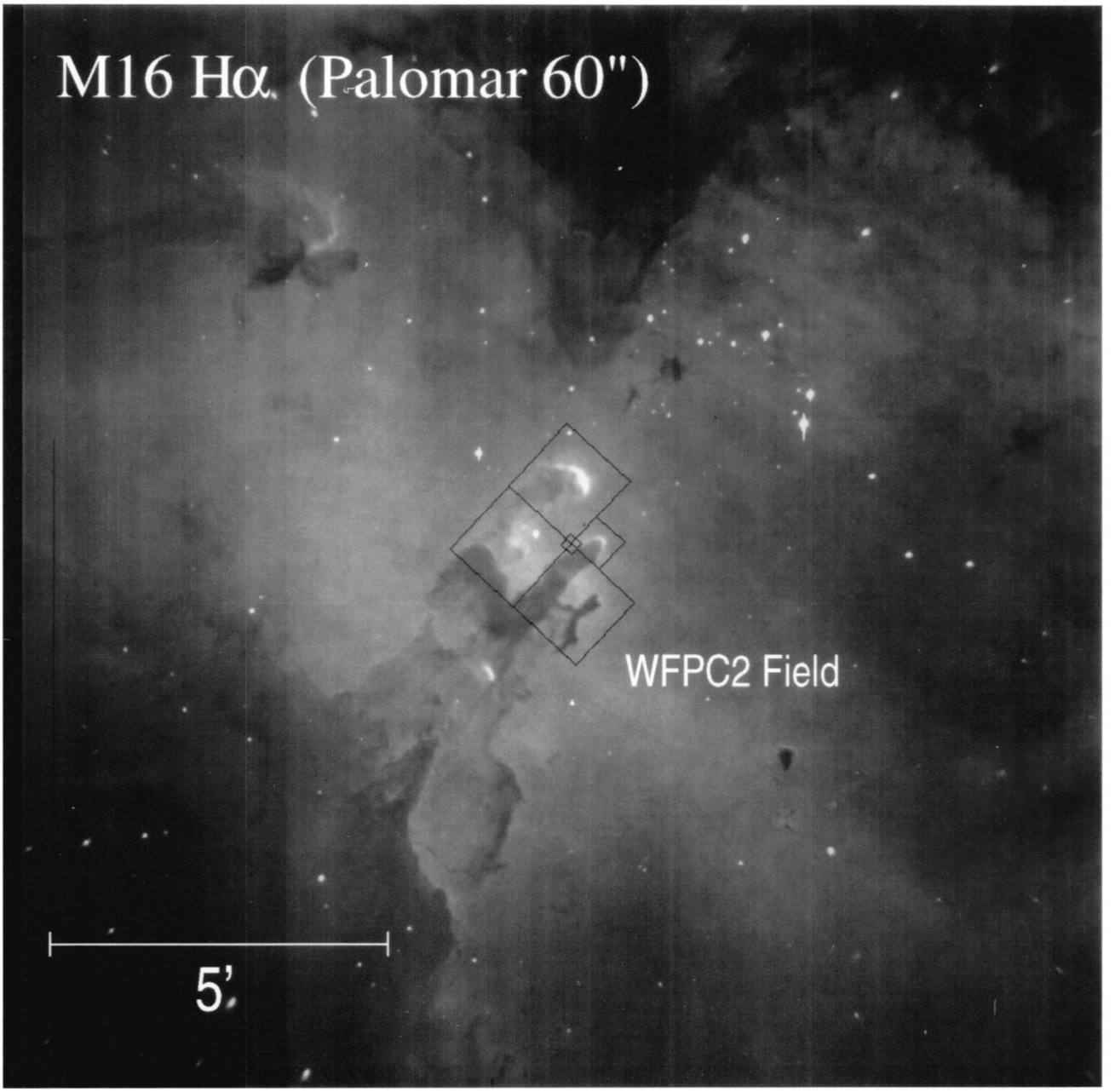

FIG. 1. Ground-based Hα image of M16 showing the field observed with WFPC2. North is at the top and east is to the left. The bar shows a length of 5′ which is $\sim 9 \times 10^{18}$ cm at a distance of $\sim$2000 pc.

Hester *et al.* (see page 2350)

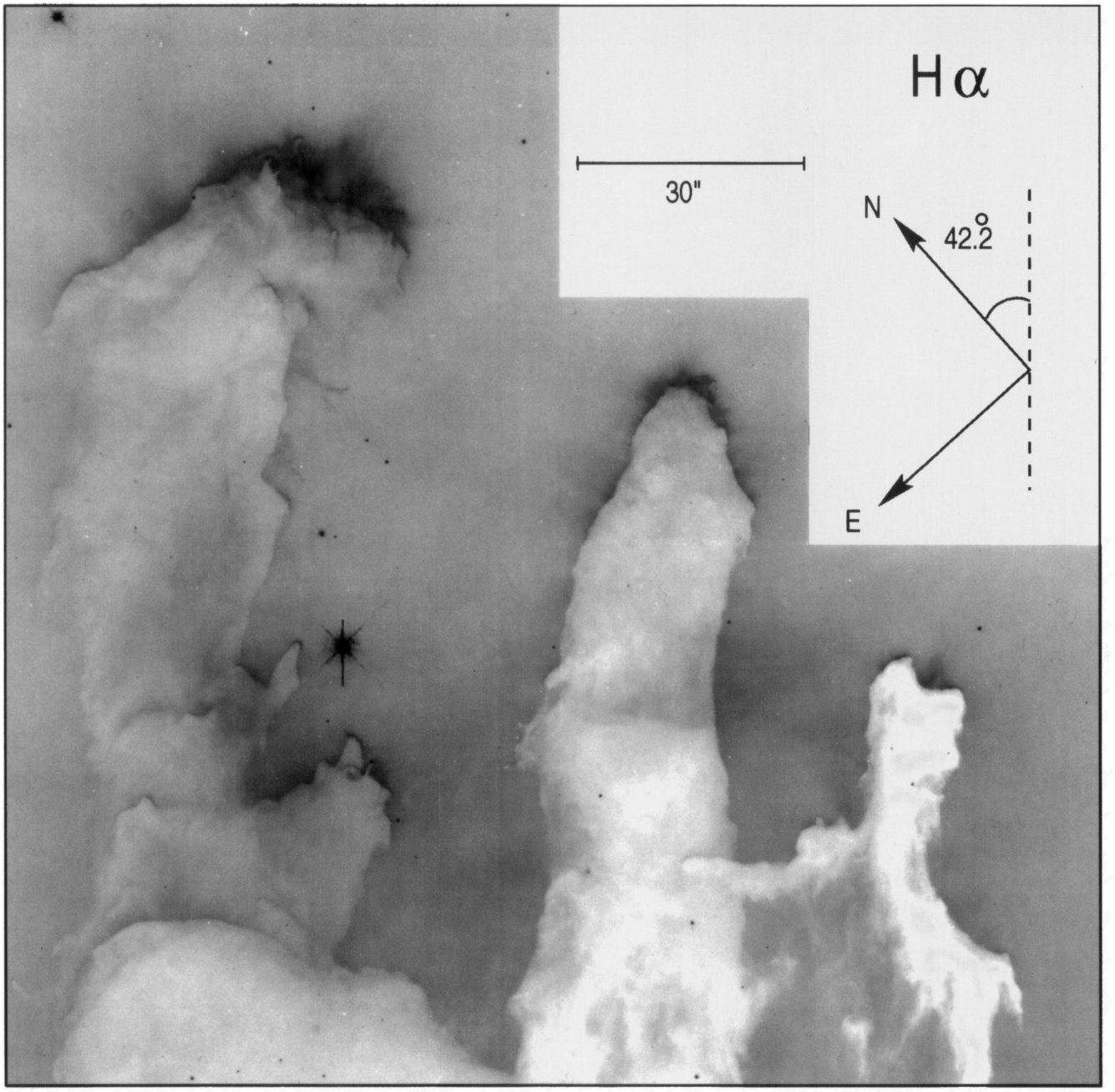

FIG. 2. WFPC2 image of elephant trunk structures in M16 taken through the F656N filter, which isolates light from Hα λ6563. The arrows indicate north and east. The bar has a length of 30″, corresponding to 9×10^{17} cm at the assumed distance of M16. The negative display uses a square root stretch.

Hester *et al.* (see page 2351)

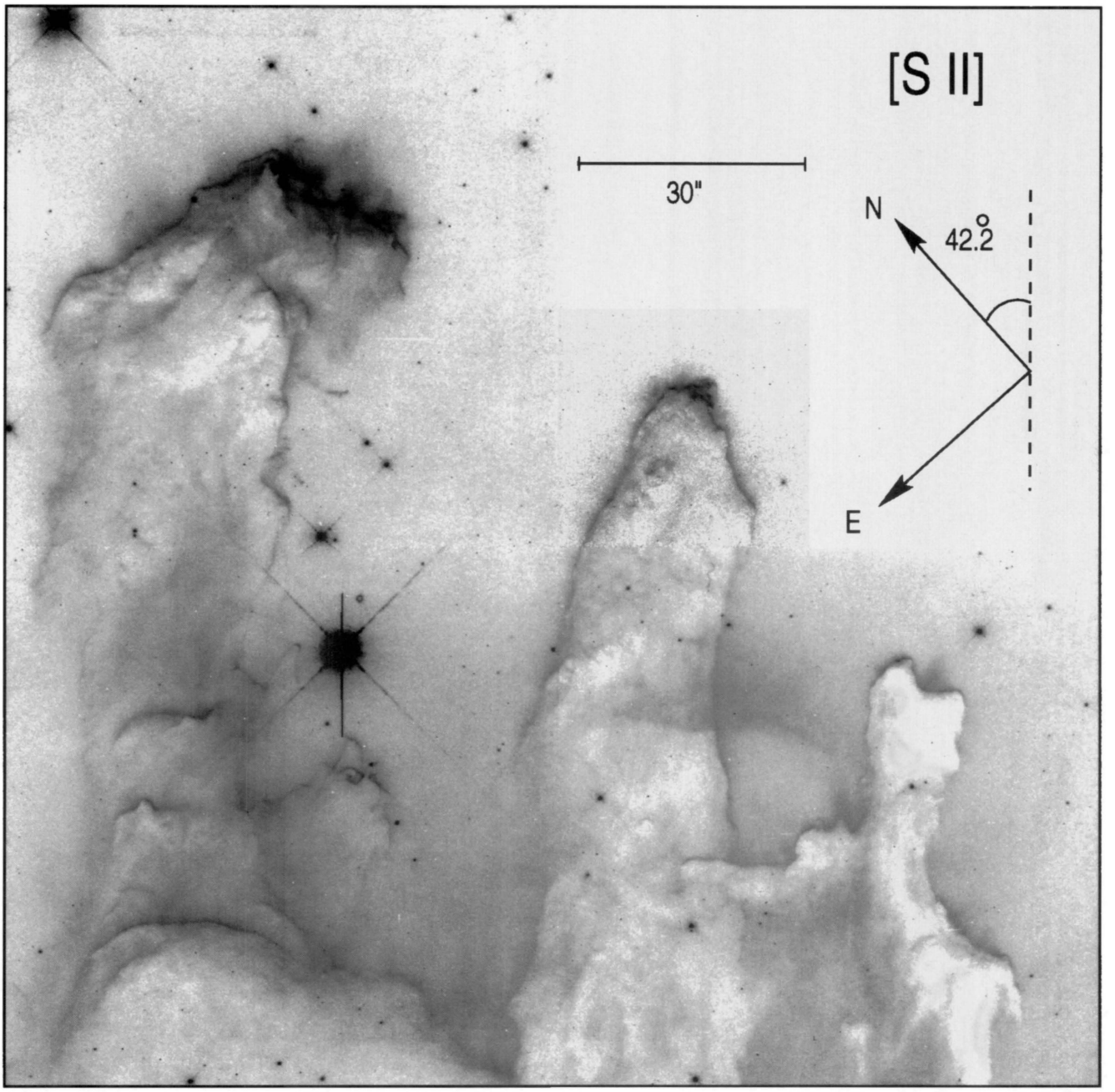

FIG. 3. WFPC2 image of elephant trunk structures in M16 taken through the F673N filter, which isolates light from [S II] λλ 6717,6731. The display uses a square root stretch.

Hester *et al.* (see page 2351)

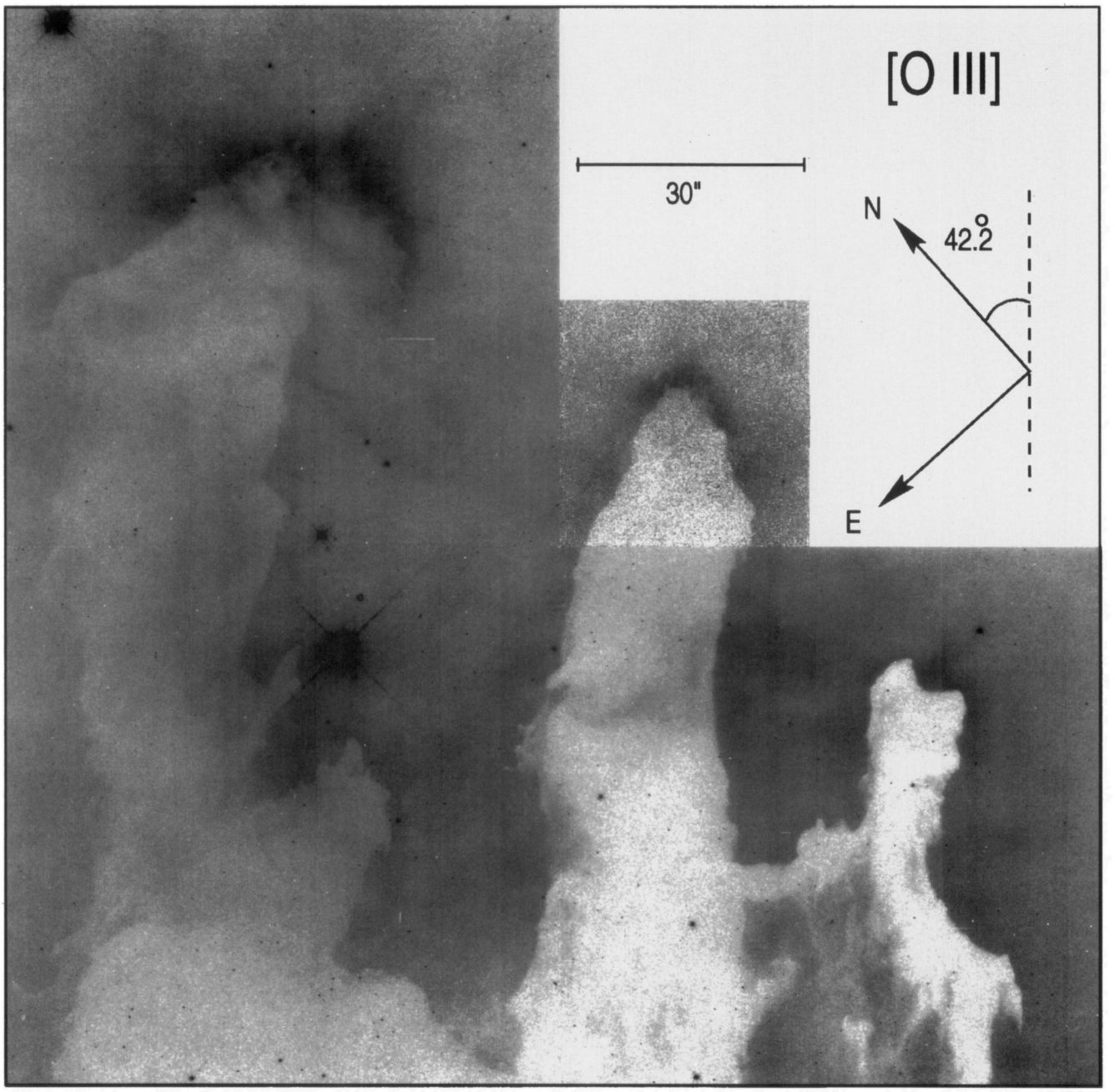

FIG. 4. WFPC2 image of elephant trunk structures in M16 taken through the F502N filter, which isolates light from [O III] λ5007. The display uses a square root stretch.

Hester *et al.* (see page 2351)

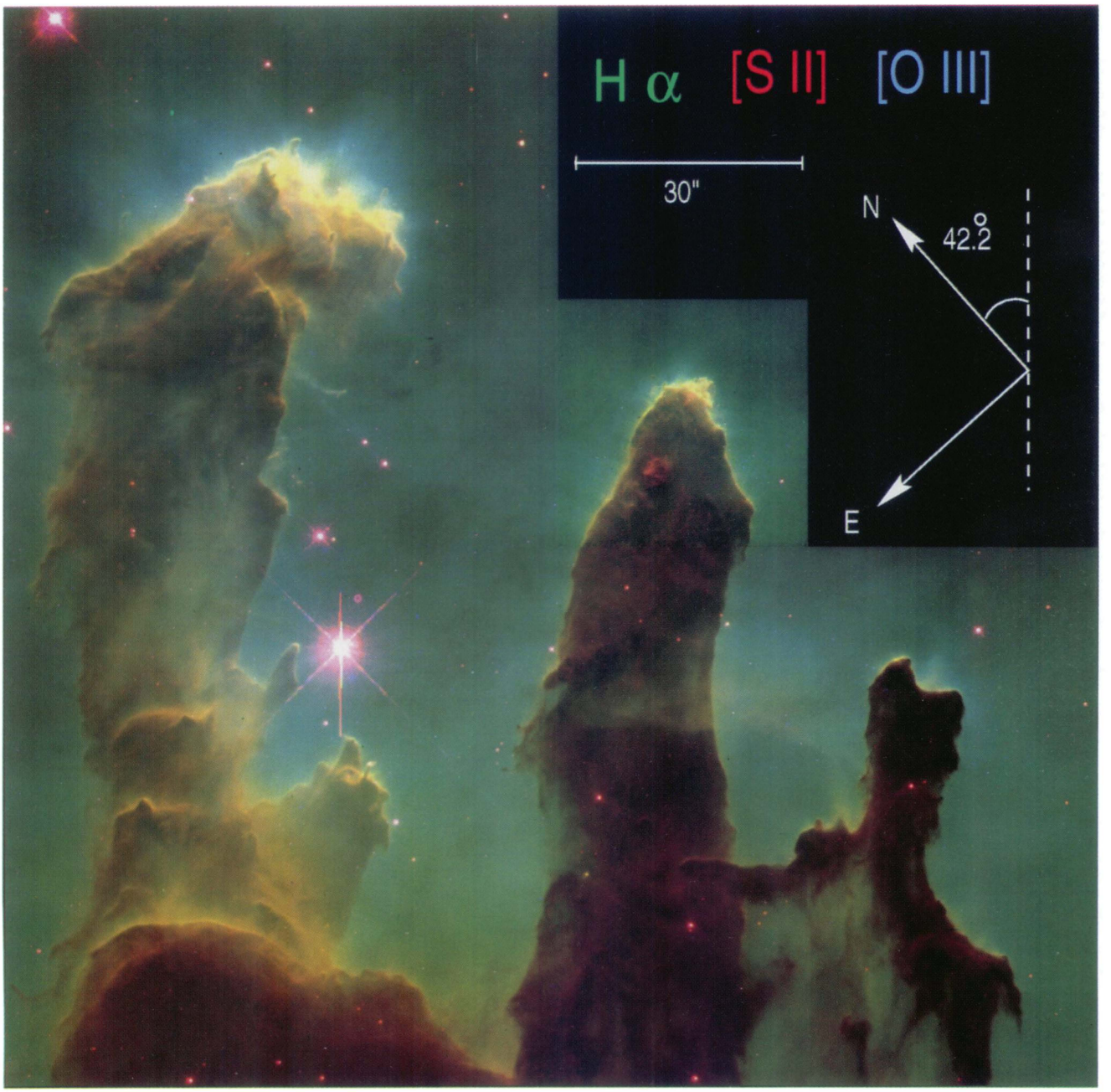

FIG. 5. Color composite of the WFPC2 images of M16. Red shows emission from [S II]. Green shows emission from Hα. Blue shows emission from [O III].

Hester *et al.* (see page 2351)

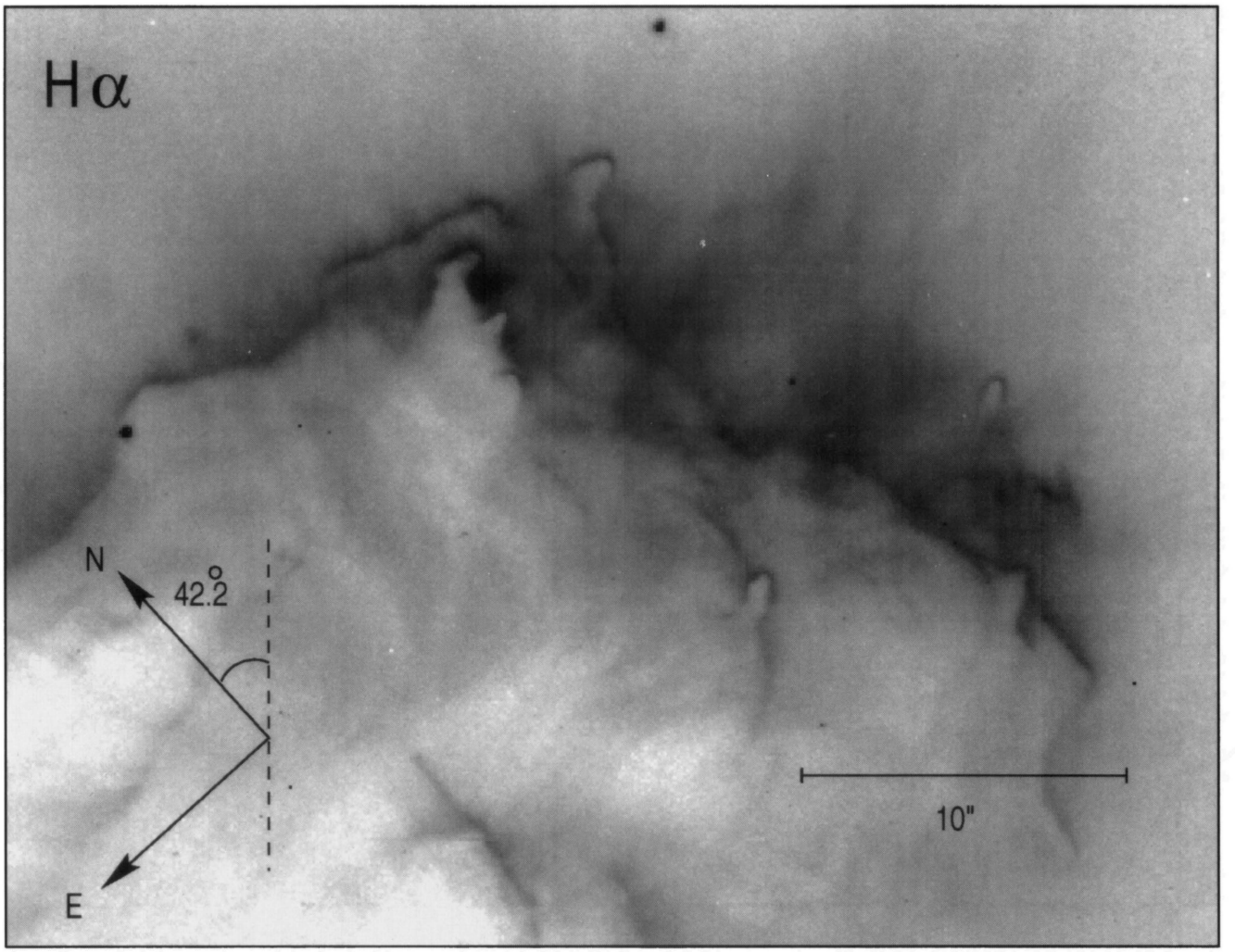

FIG. 6. An enlargement of the WFPC2 Hα image of the head of column I in M16. The 10″ bar corresponds to 3×10^{17} cm. Note both the wispy, striated texture of the photoevaporative flow and the large number of evaporating gaseous globules (EGGs) along the boundary of the molecular cloud. This entire region shows strong K-band emission.

Hester *et al.* (see page 2351)

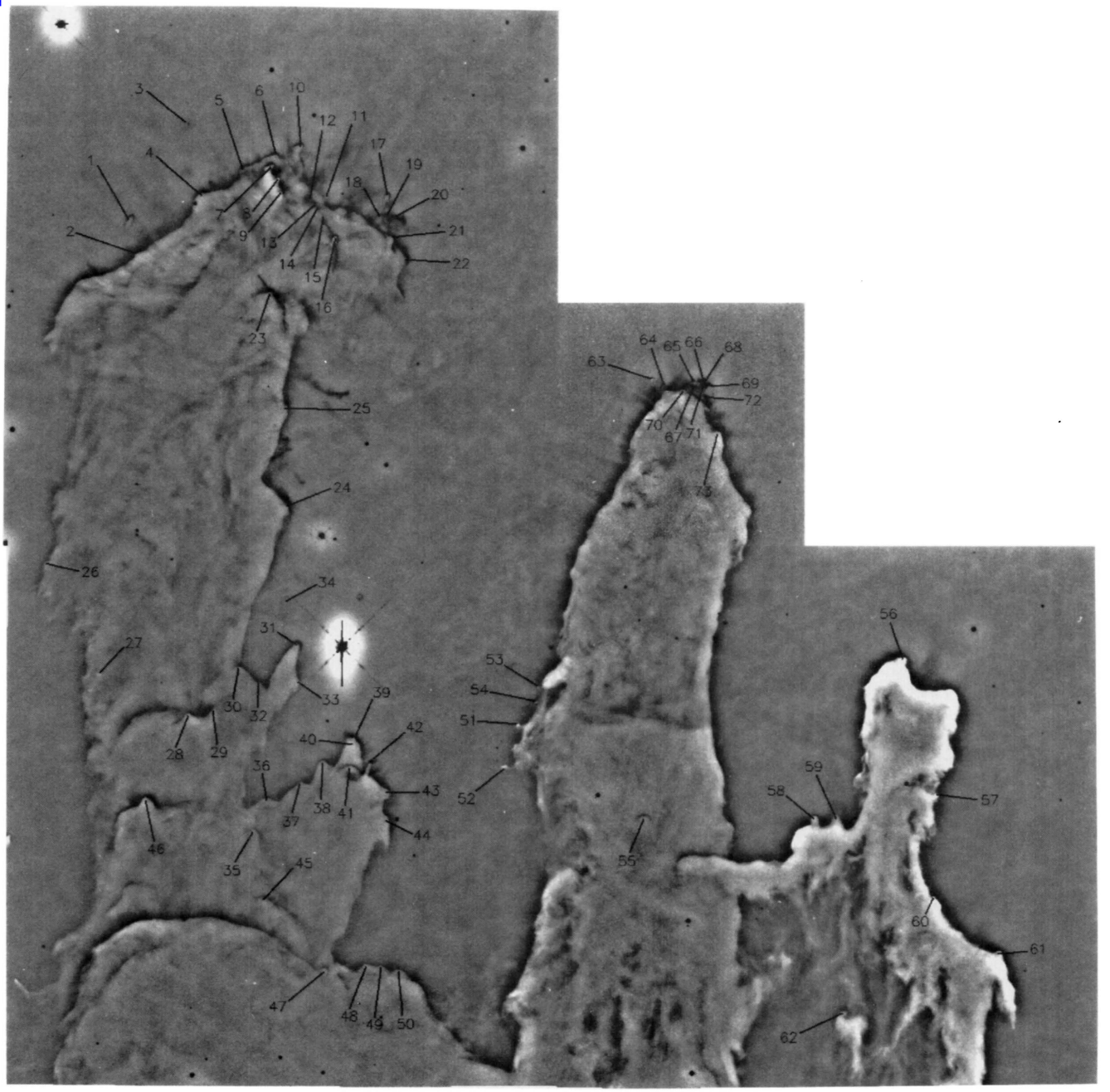

FIG. 8. A high pass filtered version of the *HST* image of M16 showing the identification of over 70 evaporating gaseous globules, or EGGs. These objects are referred to in the text using the nomenclature "M16-E*n*," where *n* is the identification number from this figure.

Hester *et al.* (see page 2354)